Journal of Materials Chemistry A

Accepted Manuscript

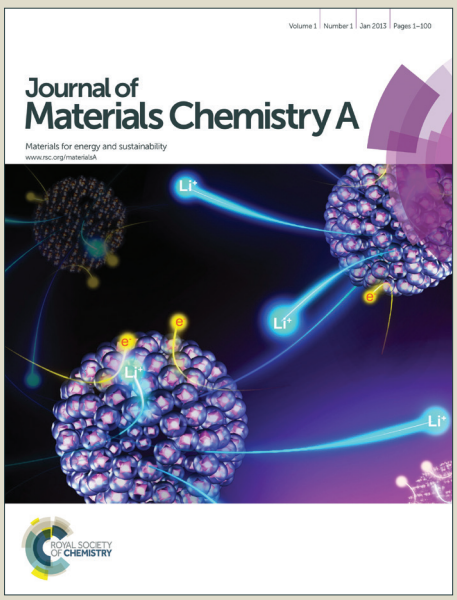

ROYAL SOCIETY OF CHEMISTRY

www.rsc.org/materialsA

Journal of

Materials Chemistry A

RSCPublishing

ARTICLE

Gold Nanoparticle-Catalysed Photosensitized Water Reduction for Hydrogen Generation

Donghua Li,[1,2] Jean-François Wehrung[1] and Yue Zhao[1,*]

Cite this: DOI: 10.1039/x0xx00000x

Received ooth January 2014,
Accepted ooth January 2014

DOI: 10.1039/x0xx00000x

www.rsc.org/

The use of gold nanoparticles (AuNPs) as a catalyst in the photosensitized water reduction for hydrogen generation was investigated using the conventional three-component systems. Three photosensitizers, ZnPP, ZnTPP and Eosin Y, were utilized to prepare water splitting solutions containing AuNPs (2 nm or 6 nm in diameter), redox mediator ($Rh(bpy)_3Cl_3$), sacrificial electron donor (TEOA) and an amphiphilic diblock copolymer, PAA_{52}-*b*-$P4VP_{90}$, whose micelles can solubilize the hydrophobic ZnPP or ZnTPP. It was found that AuNPs exhibit a good catalytic activity comparable to a Pt catalyst (K_2PtCl_4). Under visible light irradiation at room temperature, the hydrogen evolution was observed over the investigated period of time up to 10 hours, with the accumulative amount of the gas influenced by the size of AuNPs (more efficient with the 2 nm AuNPs) and the nature of the photosensitizer (comparable performance with ZnPP and Eosin Y, but lower with ZnTPP). Moreover, absorption and emission spectral changes of ZnPP in the water splitting solution were monitored and analysed; an unidentified species formed at the beginning of irradiation appears to not interfere with the photosensitized hydrogen generation process. This study suggests that AuNPs could be used to replace Pt in catalysing the photosensitized water reduction reaction in the widely adopted three-component water splitting systems.

Introduction

Secure, clean, and renewable energysourcesare needed to overcome the shortage of fossil fuels and the increasing energy consumption. Since Sun is a renewable energy source and hydrogen fuel presents itself as a clean energy, numerous research works have been carried out for the conversion of solar energy to hydrogen via photosensitized water splitting. One of the many methods consists in using photosensitized water reduction to produce H_2.[1-8] Generally, three-component systems contain a photosensitizer, a redox mediator, and a catalyst, while a sacrificial electron donor is also used to reduce the photooxidized sensitizer.[5] Part of the research effort in recent years has been dedicated to the development of new and efficient catalysts that carry out the reduction of protons to hydrogen. Examples include cobalt complexes,[9-10] iridium complexes [7] and platinum (Pt salt or Pt nanoparticles) that is the most used catalyst.[1, 11-16] Although gold is generally regarded as an inactive metal, gold nanoparticles (AuNPs) may exhibit high catalytic activity or enhance the activity.[17-19] To this regard, a number of inorganic systems with AuNPs deposited on, for example, TiO_2 [6, 20-21] and graphic carbon nitride[22] were prepared and shown to display highly efficient catalytic activity in photosensitized water splitting. By contrast, fewer organic AuNP-based catalytic systems are known to date. Alvaroet al. reported good photoinduced water splitting performance by chemically linking the photosensitizers to AuNPs either with or without an electron mediator such as methyl viologen in the solution.[23] However, to our knowledge, the catalytic property of AuNPs in the conventional, and most common, three-component systems for photosensitized water reduction leading to hydrogen has rarely been demonstrated.

On another front, it is known that the lack of water solubility can be problematic for some photosensitizers such as metal-porphyrin complexes. These are long wavelength absorption dyes and would be highly efficient for harvesting the solar energy; but the aggregation of the dyes due to low water solubility would highly quench the triplet state, which hinders the electron transfer necessary for reducing the water molecules. Therefore, many works were focused on the synthesis of effective photosensitizers bearing cation/anion[12-13, 24], or self-assembled to metal-organic framework[13] or by encapsulation[14]and so on[3, 15, 25-26] to improved water solubility. For instance, zinc(II) protoporphyrin IX (ZnPP) was encapsulated in human serum albumin, a water-soluble plasma protein, and the photosensitized water splitting could be

performed at higher concentrations of ZnPP.[14] But the drawback is the high cost of the protein[14] or hydrogenase.[26] To address this issue, in a previous study,[27] we showed that water-insoluble ZnPP could be loaded in low-cost micelles of an amphiphilic diblock copolymer of poly(acrylic acid) and poly(4-vinylpyridine) (PAA_{52}-*b*-$P4VP_{90}$) through the axial coordination between Zn and the pyridyl group, making possible the photosensitized water reduction using the conventional three-component system with Pt as the catalyst.

Being motivated by the interest of exploiting AuNPs as catalyst,[28] for photosensitized water splitting, we carried out a study using AuNPs (about 2 nm or 6 nm in diameter) as the catalyst, instead of Pt, for photosensitized water splitting, combining several photosensitizers solubilized by PAA_{52}-*b*-$P4VP_{90}$ micelles, an electron mediator (rhodium trisbipyridine chloride: $Rh(bpy)_3Cl_3$) and a sacrificial electron donor (triethanolamine: TEOA). The results reported in this paper show that AuNPs could replace Pt for catalyzed photosensitized water splitting, with a very good hydrogen generation performance.

Experimental

Details on the synthesis and characterization of the materials used in this study are presented in Supporting Information. Applying a method in the literature,[28-29] two sizes of glutathione-capped AuNPs (2 and 6 nm in diameter) were prepared and used to investigate the size effect on the catalytic efficiency. The surface plasmon resonance (SPR) peaks of the 2 nm and 6 nm AuNPs are at 523 nm and 528 nm, respectively; and the TEM images indicate that the two sizes of AuNPs are 2.0±0.7 nm and 6.0±1.0nm (Figs. S1 and S2). Meanwhile, the concentration of Au atoms in the used AuNPs catalyst solution was 12.5 mM as determined by ICP-MS. The micelle-forming diblock copolymer PAA_{52}-*b*-$P4VP_{90}$ used to solubilize various photosensitizers, was synthesized using the atom transfer radical polymerization (ATRP) method.[30] The diblock copolymer sample PAA_{52}-*b*-$P4VP_{90}$ contains about 52 units of acrylic acid and 90 units of 4-vinylpyridine. Most of the other compounds used in this study were purchased from commercial sources and used without further purification.

To prepare the water splitting solution, ZnPP (or another photosensitizer), PAA_{52}-*b*-$P4VP_{90}$ and TEOA were added to a glass vial containing ca. 9 mL ultrapure water, and stirred overnight until ZnPP was dissolved. After adjusting the pH of the solution to 7.5±0.1 by 0.1 N H_2SO4, concentrated phosphate buffered solution, $Rh(bpy)_3Cl_3$ and bipyridine (bpy) were successively added to the solution under stirring until the complete dissolution of bpy. Afterwards, the AuNPs catalyst (either 2 nm or 6 nm) was added into the solution and the weight of the solution was adjusted to 10 g by adding ultrapure water under stirring for 20 min. The final concentrations of the water splitting solution were 2 mg/mL PAA_{52}-*b*-$P4VP_{90}$, 0.1 mM ZnPP, 2 mM $Rh(bpy)_3Cl_3$, 3 mM bpy, 0.3 M TEOA, 10 mM phosphate buffer at pH=7.5 and a given AuNPs concentration. Throughout this study, only the AuNPs catalyst and its concentration were varied while all the other componentsand their concentrations in the water splitting solutions were kept the same.

For the measurement of photo-generated hydrogen, each water splitting solution was first bubbled by N_2 for 20 min to remove dissolved oxygen, and then transferred to a cell for exposure to light (the volume of the cell is ca. 8.5 mL, see Fig. S3). The solution was exposed to steady-state irradiation at 25 ^oC, using the light from a xenon lamp (1000 Watt Xenon Short Arc Lamp, Ozone Free, Oriel Instruments) with a lamp housing, a power supply and a series of filters to simulate the solar energy at the surface of earth. Those filters included a heat trap (Oriel Instruments), a long-wave pass filter (410-1200 nm, Newport, 10LWF-400-B), Am0 (Sl04486 Lot#5009, 2"×2") and Am1.5 (SL04204 Lot#2210, 2"×2"). And the irradiation intensity of the light at the cell was 150 mW/cm^2, which was measured by an optical power meter/energy meter (Newport, 1918-R) coupled with a silicon photodetector (Newport, 400-1100 nm, 918D-SL-OD3).

The volume of gas generated by the AuNP catalysed photosensitized water splitting could be obtained by measuring the volume increase of the solution with bubble. The irradiation cell was shown in Fig. S3; with gas generated, the liquid level in the pipe goes down, so that the volume increase of the solution with bubble can be measured. Meanwhile, the amount of H_2 in the gas was confirmed by GC. After a certain time of irradiation, the gas generated was collected by a gastight syringe (Series A-2, Valco Instruments) and injected into the gas chromatograph with column packed with 2 meter 5 Å molecular sieves and equipped with a TCD detector (Hewlett Packard 5890 Series II).

Results and Discussion

Basically the three-component photosensitized water reduction system involves two cycles: dye cycle and rhodium cycle.[2,5,12,14-15] The mechanism of our system is depicted in Scheme 1. First, based on the previous studies,[27, 30] the diblock copolymer PAA_{52}-*b*-$P4VP_{90}$ could form micelles with hydrophobic P4VP core and hydrophilic PAA corona. Consequently, water-insoluble dye molecules, such as ZnPP, are solubilized by the PAA_{52}-*b*-$P4VP_{90}$ polymer micelle to form the ZnPP-Polymer complex through axial coordination between Zn and the pyridyl group, as shown in Scheme 1. The latter goes to the excited state ($ZnPP^*$-Polymer) upon absorption of a photon and relaxes to the long-lived triplet state, from which electron transfer to rhodium occurs. And the $ZnPP^+$-Polymer is reduced by the electron donor to recover ZnPP-Polymer, which closes the dye cycle. For the rhodium cycle, $Rh(bpy)_3^{3+}$is first reduced to $Rh(bpy)_3^{2+}$ by $ZnPP^*$-Polymer and then reduced by another $ZnPP^*$-Polymer before being coordinated to H^+. Finally, the Rh(I) complex oxidation is attendant to the hydrogen generation at the AuNPs catalyst surface to return to $Rh(bpy)_3^{3+}$, which completes the cycle.

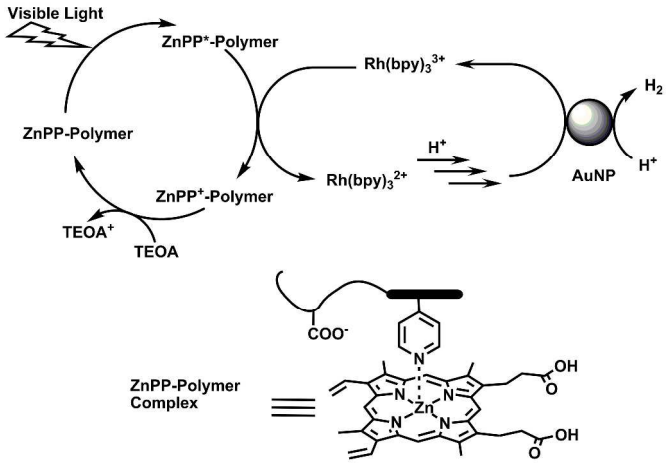

Scheme 1. Diagram for photosensitized water reduction for hydrogen evolution catalysed by gold nanoparticles (AuNPs).

TEM analysis found that the polymer formed spherical micelles with an average diameter *ca*. 20 nm (Fig. 1a). In a test, after 10 h light exposure of the solution, the morphology and size of the micelles did not display any significant changes (Fig. 1b). This result indicates that the polymer micelles are stable during the light exposure and photosensitized photochemical reaction. From the TEM image (Fig. 1b), it can also be noticed that AuNPs are not loaded in or attached onto the polymer micelles. This is reasonable considering that the isoelectric point of the GSH ligand on AuNPs is 5.02 and the pKa of carboxyl group in PAA are around 4. Under the used conditions at pH 7.5, both AuNPs and the micelles bear negative charges on surface and the electrostatic repulsion should keep them away with each other.

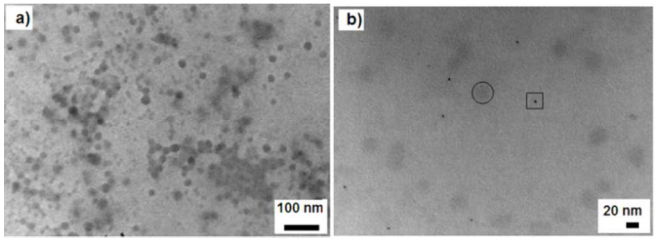

Figure 1. TEM images of a) PAA_{52}-*b*-$P4VP_{90}$ micelles and b) the water splitting solution containing 125 μM AuNPs (2 nm) after 10 hours light exposure (a micelle and an AuNP are marked by circle and square, respectively).

The catalytic efficiency of the 2nm AuNPs for hydrogen generation upon photoinduced water reduction was first investigated. The formation of H_2 due to the presence of AuNPs was first confirmed by visual observation. As shown by the photos in Figure 2, no gas bubbles could be observed with the water splitting solution containing no AuNPs even after 3h light exposure (Fig. 2a). By contrast, when the solution containing 125 μM AuNPs was irradiated by visible light for only 15 minutes, gas bubbles were generated and could be collected in the pipe (Fig. 2b). The two experiments were conducted under exactly the same conditions (water splitting solution and light irradiation) except the absence or presence of AuNPs in the solution. As mentioned above, the gas produced upon irradiation for a given time could be collected and analysed by means of GC-TCD. Compared with the H_2 standard sample, almost all the gas was hydrogen only with a few water vapours (<2%).

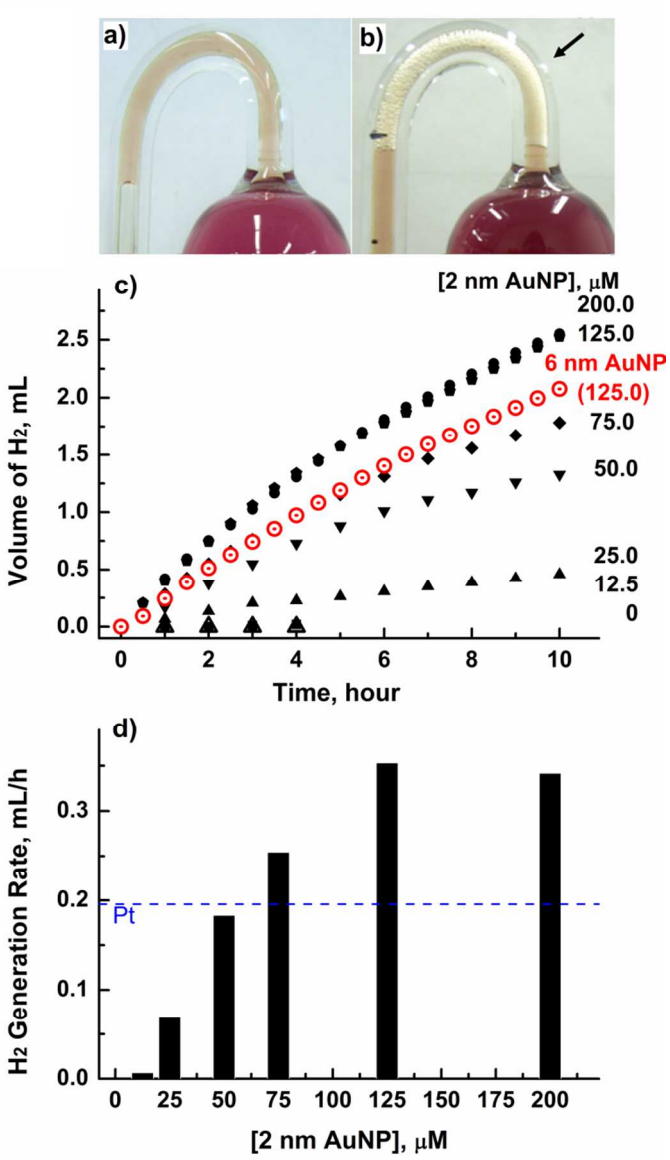

Figure 2. a) Photo of the water splitting solution without AuNPs after 3h irradiation. b) Photo of the solution containing 125 μM AuNPs (2nm) after 15 min irradiation (the arrow indicates H_2 bubbles in the pipe). c) Accumulative quantity of the H_2 generation from various water splitting solutions as a function of irradiation time, catalysed by AuNPs (2 nm with different concentrations and 6 nm at one concentration). d) H_2 generation rate in the first 3 hours of irradiation for the water splitting solutions catalysed by 2 nm AuNPs of different concentrations and, for comparison, by 200 μM K_2PtCl_4 (Pt).

The accumulative quantity of the H_2 generation over light exposure time for the water splitting solutions with different AuNPs concentrations was then measured and the results are

presented in Fig. 2c. As is seen, at the used lowest AuNPs concentration of 12.5 μM, almost no hydrogen was obtained (similar to the solution without any AuNPs). By increasing the AuNPs concentration to 25 μM, an appreciable amount of H_2 appeared. Over the 10 h irradiation period, the quantity of photo-generated H_2 increased steadily with increasing the concentration of AuNPs until 125 μM, over which no significant difference in the amount of H_2 could be observed. Also shown is the result obtained with the 6 nm AuNPs at a concentration of 125 μM. It appears that the catalytic efficiency of the larger AuNPs is lower than the smaller ones. In all cases, the hydrogen formation seems to be faster at the early time, especially within the first 3 hours over which the amount of H_2 increases nearly in a linear fashion over the irradiation time. Figure 2d shows the hydrogen formation rate (mL/h) within the first 3 hours, obtained from the slopes of the curves in Figure 2c, as a function of the AuNPs concentration. The highest rate was obtained with 125 μM AuNPs. For comparison, the rate of hydrogen formation measured with 200 μM K_2PtCl_4, which is a common catalyst, under the same conditions is also indicated in Figure 2d. Although a large amount of gold atoms in the nanoparticles may not directly perform any catalytic role, the AuNPs are still more efficient for catalysing the photosensitized water splitting than K_2PtCl_4. It can be seen that in the first 3 hours of irradiation, the accumulative amount of hydrogen catalysed by even 50 μM AuNPs is comparable to that catalysed by 200 μM K_2PtCl_4.

From Figure 2c, it is seen that the hydrogen formation rate gradually decreases over light exposure time. A series of comparative measurements were carried out using 125 μM of 2 nm AuNPs, 125 μM of 6 nm AuNPs and 200 μM of K_2PtCl_4. For each water-splitting solution, the amount of H_2 was monitored by measurement for every 15 min of irradiation. In Figure 3, the rate (the slope from the curve) is plotted *vs*. light exposure time for the three solutions. The Pt and AuNPs catalysts behave differently. The hydrogen formation rate catalysed by 200 μM K_2PtCl_4 increases gradually and reaches a platform after about 3 hours of irradiation, with only slight variation within the investigated period of 10 hours. By contrast, the hydrogen formation rate catalysed by both 2 nm and 6 nm AuNPs is higher than that catalysed by K_2PtCl_4 in the first 4 hours, but the rate then gradually decreases before reaching a stable level after 6 hours irradiation, which is lower than that catalysed by K_2PtCl_4. As for the effect of the AuNP size on the catalytic efficiency, the results in Figure 3 further confirm what is revealed in Figure 2c: the larger AuNPs are less efficient for catalysing the photosensitized water reduction in the three-component system. On one hand, it is known that the chemical reaction catalysed by the nanoparticles should occur at the active sites on the surface of the nanoparticles, which are also susceptible to be deactivated in the course of the reaction.[18] A possible loss of some active sites on the AuNP surface would result in a decrease in the hydrogen formation rate in the first 6 hours. On the other hand, the smaller nanoparticles would have more active sites on their surface than the bigger ones, which accounts for the higher catalytic efficiency of the 2 nm AuNPs for water splitting as shown in Figure 2c. Therefore, these results suggest that gold nanoclusters, such as $Au_{25}(SG)_{18}$[29] would be better catalyst for the photosensitized water reduction leading to hydrogen.

It should be noted that AuNPs were utilized directly as photosensitizer to absorb the solar light through the surface plasmon resonance.[20-21,31] In that case, AuNPs need to be loaded into TiO_2 sol; and the plasmon resonance excited electrons in AuNPs are transferred to the conduction band of the adjacent TiO_2 and reduce the water to H_2. A primary condition for the electron transfer to happen is an intimate contact of AuNPs and titania that induces a shift of the conduction band of the semiconductor toward more negative potentials at the interface.[21] This condition, obviously, is not fulfilled in the present study, since AuNPs are not in contact with any electron acceptor or semiconductor. Nevertheless, we carried out a control experiment to rule out the possibility of having AuNPs

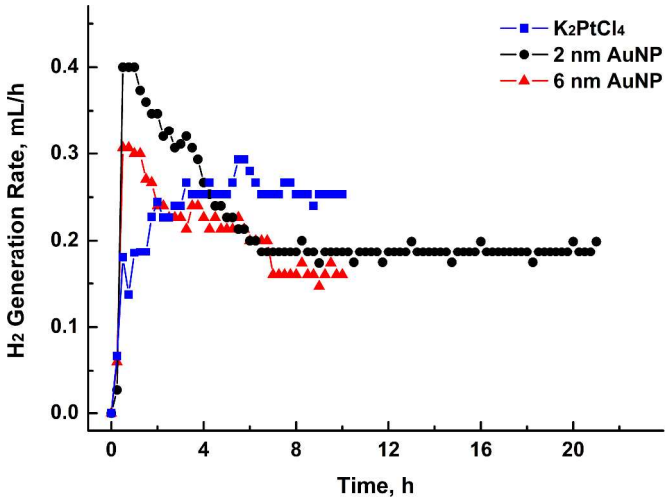

Figure 3. Variation of the H_2 generation rate over irradiation time for the water splitting solutions catalyzed by 125 μM 2 nm AuNPs, 125 μM 6 nm AuNPs and 200 μM K_2PtCl_4 (Pt).

act as the photosensitizer to absorb the visible light and transfer the electron for hydrogen generation. With a water splitting solution containing 125 μM of AuNPs (2 nm) but without any ZnPP, no gas was observed after continuous irradiation for 3 hours (Fig.S3). Moreover, three separate experiments using 125 μM AuNPs (2 nm) were performed, and the results on the catalytic efficiency of AuNPs in photosensitized water splitting with the used system are quite reproducible (Fig.S4). The derivation of the hydrogen generation rate or the accumulative amount is generally lower than 20 %.

The absorption and emission spectral properties of the photosensitizer ZnPP in the water splitting solution before and after light exposure were investigated. It is well-known that the absorption spectrum of ZnPP in THF solution has two features corresponding to one symmetry-allowed transition (Soret band or B(0,0) band at 420 nm) and two symmetry-forbidden transitions (Q(1,0) and Q(0,0) band at 545 nm and 580 nm, respectively).[32-33] From the absorption and emission spectra in

Figure 4, it is seen that the Q bands of ZnPP in the water splitting solution containing 200 μM AuNPs (2nm) appear at 553 nm and 590 nm with large bathochromic shift. For comparison, the absorption spectrum of 200 μM AuNPs alone is also shown, and the absorbance of the catalyst is negligible in the Q bands region of ZnPP. On the other hand, the strong and sharp emission peaks at 600 nm and 645 nm with a mirror image of the Q bands in absorption spectrum can be assigned to dissolved ZnPP.[33] Before irradiation, all the absorption and emission spectra of the water splitting solutions containing AuNPs of different concentrations or K_2PtCl_4 are similar. Those spectra indicate that the hydrophobic ZnPP photosensitizer is well solubilized by the polymer micelles through the axial coordination between pyridine and ZnPP,[14, 27, 34] as revealed by the large shift of the Q bands. After irradiation for 10 hours, absorption and emission spectra changes were observed. The Q bands of ZnPP in the absorption spectrum are hypsochromically shifted to 546 nm and 581 nm, respectively, and accompanied by a new peak appearing at 636 nm. Meanwhile the emission peak at 600 nm shifts to 592 nm and decreases in intensity, while the emission peak intensity at 646 nm decreases by a much lesser extent. And the excitation spectrum of the water splitting solution after irradiation also displays a new excitation peak at 636 nm, the same wavelength as that in the absorption spectrum (Fig. S5 and Fig. 4). Similar spectral changes were observed for all water splitting solutions (Figs. S6 and S7). In another control test, the spectral evolution versus irradiation time was monitored for a solution containing only ZnPP, polymer and TEOA at pH 7.5 but without the redox mediator and catalyst (Fig. S8). It was found that the new absorption peak at 636 nm actually appeared quickly upon irradiation, within the first 4 minutes, with the concomitant quenching of the emission at 600 nm. And the continuing irradiation for prolonged times only resulted in modest changes in the absorption and emission spectra of ZnPP. Therefore, it appears that the spectral change is not caused by the presence of the AuNPs catalyst or the redox mediator in the water splitting solution, and is not interfering with the photosensitized water reduction reaction.

There are many possible reasons for the observed spectral changes upon irradiation, such as photo-decomposition of ZnPP, or photochemical reaction with ZnPP.[35, 36, 37] It is known that ZnPP could be decomposed, especially in acid environment, to zinc ion and protoporphyrin (PP). To examine this possibility, we prepared a water splitting solution containing 0.1 mM PP and 125 μM AuNPs (2 nm), and found that the hydrogen amount generated after 6 h continuous visible light irradiation was very low, *ca*. 20 μL, which was about 2% of what was obtained with ZnPP under the same conditions. From this control experiment, the photo-decomposition of ZnPP or ZnPP-polymer complex can be ruled out. It is likely that the spectral changes could be due to the photooxidation of ZnPP under irradiation,[36,37] but at this time, the actual photoproducts remain unclear.

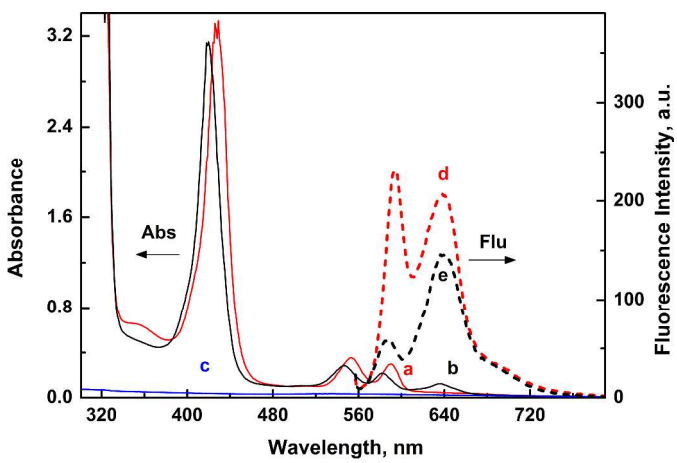

Figure 4. Absorption (solid line, 0.2 cm optical length) and emission (λ_{ex}= 550 nm, dash line) spectra of the water splitting solution containing 200 μM AuNPs (2 nm) before (a, d, in red line) and after (b, e, in black line) irradiation for 10 hours, and the absorption spectrum of 200 μM AuNPs (2 nm) in H_2O (c).

Finally, we investigated the generality of using AuNPs as the catalyst for photosensitized water reduction in the three-component systems by using two other photosensitizers, zinc tetraphenylporphyrin (ZnTPP) and Eosin Y, while keeping all other conditions unchanged unless otherwise stated. The solubility in water of ZnTPP is lower than ZnPP due to the hydrophobic groups on porphyrinring, but the solubility can be improved by the diblcok copolymer micelles via the same axial coordination between pyridine and zinc in ZnTPP. The water solubility of Eosin Y is much better than both ZnPP and ZnTPP, while there is no axial coordination between the polymer and Eosin Y (chemical structure in Fig.5). It should be noted that Eosin Y as photosensitizer in MeCN-H_2O mixture exhibits very good hydrogen generation performance.[38] In the present study, the water splitting was carried out in pure water. Hydrogen generation with both ZnTPP and Eosin Y as a result of the AuNPs catalysed photosensitized water reduction was observed. The accumulative amounts of H_2 formed in the water splitting solution containing 125 μM AuNPs (2 nm) over 6 hours of light exposure are shown in Figure 5, together with the data obtained with ZnPP for comparison. With ZnTPP, the hydrogen generation increases continuously under irradiation, but the amount of H_2 is much smaller than that obtained with ZnPP (about a quarter). In the water splitting solution, ZnTPP solubilized by the polymer micelles displays prominent Q bands at 565 nm and 605 nm in the absorption spectrum and two emission peaks at 618 nm and 663 nm in the emission spectrum (Fig. S9a). After irradiation for 6 hours, only some decrease in absorbance and bathochromic shift in emission were observed. In the case of Eosin Y, when dissolved in the water splitting solution with polymer micelles, the absorption peak displays a bathochromic shift to 534 nm, and the emission peak appears at 575 nm (Fig. S9b). Such red shifts for the absorption and emission imply changes in the microenvironment of the Eosin Y dye molecules. After

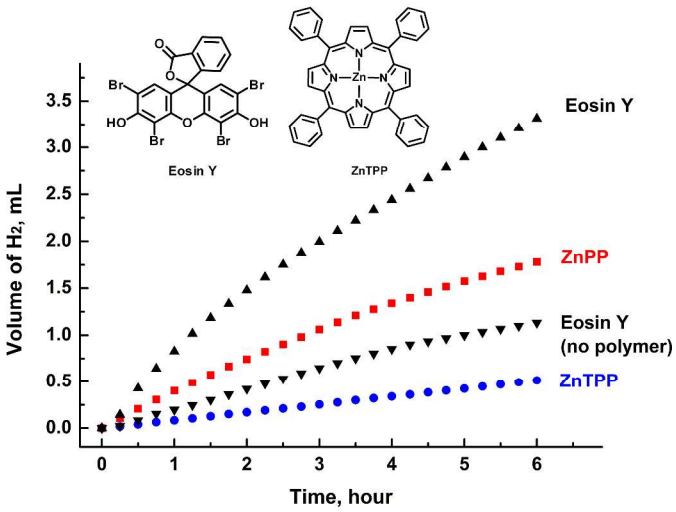

Figure 5. Accumulative quantity of the H_2 generation from the water splitting solution using either Eosin Y, ZnTPP or ZnPP as photosensitizers and catalysed by 125 µM 2 nm AuNPs. [PAA_{52}-*b*-$P4VP_{90}$]= 2 mg/mL; [$Rh(bpy)_3Cl_3$]= 2 mM; [bpy]= 3 mM; [TEOA]= 0.3 M; pH=7.5 (10 mM phosphate buffer) at 25°C. Photosensitizer:[Eosin Y]= 0.2 mM, or [ZnTPP]= 0.1 mM, or [ZnPP]= 0.1 mM.

irradiation for 6 hours, decrease in the absorbance and emission intensity without significant spectral shift was observed (Fig. S9b). As for the hydrogen evolution, the amount of H_2 obtained with Eosin Y as photosensitizer is comparable to that with ZnPP as photosensitizer, considering the concentration of Eosin Y was twice that of ZnPP in Figure 5. Since Eosin Y is soluble in water, we evaluated the possible role of the polymer micelle in the hydrogen evolution by using a water splitting solution without polymer (all other concentrations were the same). It was found that the amount of formed hydrogen decreased significantly in the absence of PAA_{52}-*b*-$P4VP_{90}$ (about a third of that obtained with the polymer micelle). The reason for the reduced performance seems to be the occurrence of aggregation of the dye molecules in the solution under irradiation. The absorption and emission of the dye in the solution after irradiation decreased considerably (Fig. S9c). This aggregation is also observable from visual inspection of the solution before and after irradiation (Fig. S10). With the polymer, the colour due to the absorption of Eosin Y remained after the irradiation, while without the polymer it was gone after the irradiation. These results indicate that even with the water soluble Eosin Y, the diblcok copolymer has the effect of preventing the aggregation of dye molecules under light exposure, which favours the AuNPs catalysed photosensitized water reduction for hydrogen formation.

Conclusions

We have shown that AuNPs can replace Pt as the catalyst for photosensitized water reduction leading to hydrogen generation using the conventional three-component systems. Three photosensitizers, of which two have low water solubility (ZnPP and ZnTPP) and one is water soluble (Eosin Y), were investigated in conjugation with the redox mediator ($Rh(bpy)_3Cl_3$), the sacrificial electron donor (TEOA), the PAA_{52}-*b*-$P4VP_{90}$ diblock copolymer for improving the solubility of the hydrophobic photosensitizers, and AuNPs of two different sizes (2 nm and 6 nm). The results show that under visible light irradiation, hydrogen gas can be formed over hours, and that the catalytic efficiency of AuNPs is comparable to a Pt catalyst (K_2PtCl_4). Moreover, the smaller AuNPs exhibit a higher catalytic efficiency. Of the three photosensitizers, when catalysed by the same AuNPs and under the same conditions, the water splitting solutions of ZnPP and Eosin Y gave rise to similar accumulative amounts of hydrogen, while less hydrogen was obtained with the solution of ZnTPP. It is worth mentioning that the absorption and emission spectral analysis found that at the beginning of light exposure, a new and unidentified species is formed, possibly upon the photooxidation of ZnPP, which, however, does not seem to interfere the photosensitized hydrogen generation.

Acknowledgement

YZ acknowledges the financial support from the Natural Sciences and Engineering Research Council of Canada (NSERC) and le Fonds de recherche du Québec: Nature et technologies (FRQNT). The authors also thank Opsun Technologies (Quebec) for help. YZ is a member of the FRQNT-funded Center for Self-Assembled Chemical Structures (CSACS) and Centre québécois sur les matériaux fonctionnels (CQMF).

1. Département de Chimie, Université de Sherbrooke, Québec, Canada J1K 2R1, E-mail: Yue.Zhao@usherbrooke.ca
2. R&D Center, Guangzhou Liby Enterprise Group Co., Ltd., Guangzhou, Guangdong, 510170, China

†Electronic supplementary information (ESI) available: Details on synthesis, characterization and sample preparation. See DOI: 0.1039/b000000x/

1. J. Kiwi and M. Gratzel, *Nature*, 1979, **281**, 657-658.
2. M. Kirch, J.-M. Lehn and J.-P. Sauvage, *Helv. Chim. Acta*, 1979, **62**, 1345-1384.
3. J. R. Darwent, P. Douglas, A. Harriman, G. Porter and M.-C. Richoux, *Coord. Chem. Rev.*, 1982, **44**, 83-126.
4. A. J. Bard and M. A. Fox, *Acc. Chem. Res.*, 1995, **28**, 141-145.
5. A. J. Esswein and D. G. Nocera, *Chem. Rev.*, 2007, **107**, 4022-4047.
6. A. Primo, A. Corma and H. Garcia, *Phys. Chem. Chem. Phys.*, 2011, **13**, 886-910.
7. S. Fukuzumi and T. Suenobu, *DaltonTrans.*, 2012, **42**, 18-28.
8. Y. H. Hu, *Angew. Chem. Int. Ed.*, 2012, **51**, 12410-12412.
9. V. Artero, M. Chavarot-Kerlidou and M. Fontecave, *Angew. Chem. Int. Ed.*, 2011, **50**, 7238-7266.
10. Y. Sun, J. Sun, J. R. Long, P. Yang and C. J. Chang, *Chem. Sci.*, 2012, **4**, 118-124.
11. G. M. Brown, S. F. Chan, C. Creutz, H. A. Schwarz and N. Sutin, *J. Am. Chem. Soc.*, 1979, **101**, 7638-7640.
12. K. Kalyanasundaram and M. Grätzel, *Helv. Chim. Acta*, 1980, **63**, 478-485.

13. A. Fateeva, P. A. Chater, C. P. Ireland, A. A. Tahir, Y. Z. Khimyak, P. V. Wiper, J. R. Darwent and M. J. Rosseinsky, *Angew. Chem. Int. Ed*., 2012, **51**, 7440-7444.
14. T. Komatsu, R. M. Wang, P. A. Zunszain, S. Curry and E. Tsuchida, *J. Am. Chem. Soc*., 2006, **128**, 16297-16301.
15. D. L. Jiang, C. K. Choi, K. Honda, W. S. Li, T. Yuzawa and T. Aida, *J. Am. Chem. Soc*., 2004, **126**, 12084-12089.
16. Y. Chen and P. V. Kamat,*J. Am. Chem. Soc*., 2014, **136**, 6075-6082.
17. M. C. Daniel and D. Astruc, *Chem. Rev*., 2004, **104**, 293-346.
18. P.-P. Fang, S. Duan, X.-D. Lin, J. R. Anema, J.-F. Li, O. Buriez, Y. Ding, F.-R. Fan, D.-Y. Wu, B. Ren, Z. L. Wang, C. Amatore and Z.-Q. Tian, *Chem. Sci*., 2011, **2**, 531-539.
19. W. Hou and S. B. Cronin, Adv. Funct. Mater., 2012, 23, 1612-1619.
20. Z. W. Seh, S. Liu, M. Low, S.-Y. Zhang, Z. Liu, A. Mlayah and M.-Y. Han, *Adv. Mater*., 2012, **24**, 2310-2314.
21. C. G. Silva, R. Juárez, T. Marino, R. Molinari and H. García, *J. Am. Chem. Soc*., 2010, **133**, 595-602.
22. Y. Di, X. Wang, A. Thomas and M. Antonietti, *ChemCatChem*, 2010, **2**, 834-838.
23. M. Alvaro, C. Aprile, B. Ferrer, F. Sastre and H. Garcia, *DaltonTrans*., 2009, 7437-7444.
24. E. Adar, Y. Degani, Z. Goren and I. Willner, *J. Am. Chem*. Soc., 1986, **108**, 4696-4700.
25. L. Persaud, A. J. Bard, A. Campion, M. A. Fox, T. E. Mallouk, S. E. Webber and J. M. White, *J. Am.Chem. Soc*., 1987, **109**, 7309-7314.
26. X. Li, M. Wang, S. Zhang, J. Pan, Y. Na, J. Liu, B. r. Åkermark and L. Sun, *J. Phys. Chem. B,* 2008, **112**, 8198-8202.
27. J.-F. Wehrung, D. Li, D. Han, A. Yavrian and Y. Zhao, *J. Mater. Chem. A*, 2013, **1**, 8358-8362.
28. P. Zhao, N. Li and D. Astruc, *Coord. Chem. Rev.*, 2013, **257**, 638-665.
29. Z. Wu, J. Suhan and R. Jin, *J. Mater. Chem.*, 2009, **19**, 622-626.
30. Q. Bo and Y. Zhao, *J. Polym. Sci. Pol. Chem.*, 2006, **44**, 1734-1744.
31. J.-J. Chen, J. C. S. Wu, P. C. Wu and D. P. Tsai, *J.Phys. Chem. C,* 2010, **115**, 210-216.
32. L. Luo, C.-H. Chang, Y.-C. Chen, T.-K. Wu and E. W.-G. Diau, *J.Phys. Chem. B*, 2007, **111**, 7656-7664.
33. J.-S. Lin, Y.-C. Chen, C.-C. Chen, E. W.-G. Diau and T.-F. Liu, *J. Chin. Chem. Soc.*, 2006, **53**, 201-208.
34. F. D'Souza, Y.-Y. Hsieh and G. R. Deviprasad, *Inorg. Chem*., 1996, **35**, 5747-5749.
35. M. Ethirajan, Y. Chen, P. Joshi and R. K. Pandey, Chem. Soc. Rev., 2011, 40, 340-362.
36. G. Zheng, M. Shibata, T. J. Dougherty and R. K. Pandey, J. Org. Chem., 1999, 65, 543-557.
37. L. Ma, S. Bagdonas and J. Moan, J. Photochem. Photobiol. B-Biol., 2001, 60, 108-113.
38. T. Lazarides, T. McCormick, P. Du, G. Luo, B. Lindley and R. Eisenberg, *J. Am. Chem. Soc*., 2009, **131**, 9192-9194.